BAREKENG: Journal of Mathematics and Its Applications
June 2026 Volume 20 Issue 2 Page 1485–1500
P-ISSN: 1978-7227 E-ISSN: 2615-3017
https://doi.org/10.30598/barekengvol20iss2pp1485-1500

SPATIAL EXTRAPOLATION OF MALARIA CASES IN CENTRAL PAPUA USING CO-KRIGING BASED ON RAINFALL AND OBSERVATIONAL DATA FROM PAPUA PROVINCE

Toha Saifudin[1*], Nur Chamidah[2], Azizah Atsariyyah Zhafira[3], Gabriella Agnes Budijono[4], Rivaldi Sihite[5], Mochammad Baihaqi[6], R. Arya Januarta[7]

[1,2,3,4,5,6,7]*Statistics Study Program, Faculty of Science and Technology, Universitas Airlangga*
Jln. Dr. Ir. H. Soekarno, Surabaya, 60115, Indonesia

*Corresponding author's e-mail: *tohasaifudin@fst.unair.ac.id*

Article Info

Article History:

Received: 8th June 2025
Revised: 13th July 2025
Accepted: 3rd October 2025
Available online: 26th January 2026

Keywords:

Central Papua;
Co-Kriging;
Malaria;
Rainfall;
Spatial data.

ABSTRACT

Malaria is an infectious disease that remains a significant health burden in Indonesia, particularly in Papua Province. This province has the highest malaria incidence rate nationally, influenced by various environmental factors such as rainfall. This study aims to estimate the number of malaria cases in districts/cities of Central Papua Province that do not have direct observation data, by utilizing the Co-Kriging method based on rainfall as a secondary variable and malaria cases as a primary variable from Papua Province. The secondary data used in this study were obtained from the official website of the Badan Pusat Statistik (BPS) of Papua Province, which includes the number of malaria cases in districts/cities as well as rainfall data from meteorological stations in the same region, collected in 2023. Three types of semivariogram models-spherical, exponential, and gaussian-were used to select the best model through statistical evaluation using Mean Squared Error (MSE) and Mean Absolute Percentage Error (MAPE). The results showed that the Gaussian semivariogram model provided the most optimal prediction results with an MSE of 10.895 and an MAPE of 4.67%. The estimates show that malaria cases in Central Papua are relatively uniform, with the highest incidence in Puncak Jaya district (219/1000 population) and the lowest in Mimika district (211/1,000 population). This approach is expected to be an important tool in spatially based disease planning and control and support the achievement of Sustainable Development Goals (SDGs), especially goals 3 (Good Health and Well-Being) and 13 (Climate Action).

How to cite this article:

T. Saifudin *et al*., "SPATIAL EXTRAPOLATION OF MALARIA CASES IN CENTRAL PAPUA USING CO-KRIGING BASED ON RAINFALL AND OBSERVATIONAL DATA FROM PAPUA PROVINCE", *BAREKENG: J. Math. & App.*, vol. 20, no. 2, pp. 1485-1500, Jun, 2026.

Journal homepage: *https://ojs3.unpatti.ac.id/index.php/barekeng/*
Journal e-mail: *barekeng.math@yahoo.com; barekeng.journal@mail.unpatti.ac.id*

Research Article · Open Access

1. INTRODUCTION

Malaria is an infectious disease transmitted through the bite of female Anopheles mosquitoes [1]. According to the World Malaria Report 2023, there were approximately 263 million malaria cases worldwide in 2023, with a total of 597,000 deaths, making malaria one of the most significant infectious diseases globally [2]. In Indonesia, the Ministry of Health recorded an increase in the number of malaria case examinations nationwide, reaching 3,464,738 individuals, with 418,546 confirmed positive cases in the same year. Papua Province reported the highest malaria incidence rate (Annual Parasite Incidence/API), at 156.59 per 1,000 population, far exceeding that of other provinces [3]. This condition is consistent with the large number of districts/cities in Papua that remain categorized as high-endemic areas, indicating that Papua Province contributes substantially to the national malaria burden.

The rise in malaria cases may be attributed to several factors, including environmental and weather conditions. One of the climatic factors influencing the increase in malaria incidence is rainfall levels. A study conducted in Jimma city, Southwest Ethiopia, demonstrated a significant association between climatic elements such as temperature, humidity, and rainfall with malaria incidence from 2000 to 2009 [4]. Data from a study by [5] revealed that malaria cases decreased during periods of peak rainfall, while cases increased during periods of low rainfall. Meanwhile, research by [6] showed that malaria transmission in the highlands of Kenya exhibited highly heterogeneous spatial patterns, influenced by micro-environmental factors such as altitude, proximity to water sources, and housing structures. These findings indicate that malaria tends to exhibit spatial patterns, making spatial approaches more relevant in predicting and modeling malaria cases based on contributing factors.

One relevant spatial analysis method for examining this phenomenon is Co-Kriging. Co-Kriging is a geostatistical technique that improves prediction accuracy by combining low- and high-fidelity data. It is especially efficient in high-dimensional problems due to its reduced computational cost compared to other Kriging variants [7]. In the field of epidemiology, Co-Kriging has been applied to estimate the spatial distribution of diseases by incorporating environmental variables as predictors [6]. In this case, Co-Kriging serves as a multivariate geostatistical technique capable of analyzing and predicting malaria case distributions by considering supporting variables such as rainfall. Co-Kriging allows the integration of information from two or more spatially correlated variables, yielding more accurate predictions compared to conventional single-variable interpolation methods such as ordinary kriging [8]. This has been demonstrated in previous studies, which found that Co-Kriging provides superior estimation results, particularly when correlated secondary data are used to strengthen primary data estimations [9], [10]. Thus, spatial analysis using Co-Kriging can offer a more comprehensive understanding of the relationship between malaria cases and rainfall in Papua.

The Co-Kriging method has been successfully applied in several studies related to environmental health. For instance, research by [11] demonstrated the effectiveness of the Co-Kriging method in mapping mosquito-borne disease risks such as Zika, Dengue, and Chikungunya in Colombia. In addition, a spatial study on malaria cases conducted by [12] aimed to predict malaria transmission risk in endemic regions of Iran using the Co-Kriging method. The study's findings indicated that socio-economic and climatic variables were significant factors contributing to disease transmission.

Although several studies have employed spatial approaches to examine malaria cases globally, the specific application of Co-Kriging to malaria cases in Papua Province remains very limited. Considering that Central Papua Province is a newly established administrative region that was formerly part of Papua Province, this study justifies the use of spatial data from Papua Province as a reference [13]. Therefore, this study aims to estimate (extrapolate) the number of malaria cases in districts/cities within Central Papua Province lacking data (missing values) by utilizing spatial information on malaria cases and rainfall from Papua Province. This study is expected to contribute to the formulation of malaria prevention strategies that take into account local climatic conditions and spatial analysis, particularly in Papua Province, which bears the highest malaria burden in Indonesia. Furthermore, this study aligns with the Sustainable Development Goals (SDGs), particularly Goal 3 about Good Health and Well-Being, specifically target 3.3, which focuses on preventive efforts and the control of communicable and endemic diseases such as malaria, and Goal 13 about Climate Action.

2. RESEARCH METHODS

2.1 Data and Data Sources

This study uses secondary data obtained from the official website of the Central Statistics Agency (BPS) of Papua Province (2025) [14]. The data includes malaria case counts in districts/cities across Papua Province and rainfall data from meteorological stations in the same region, collected in 2023. The data processing and statistical analysis were conducted using R statistical software [15] and Python programming language [16] to perform descriptive analysis, spatial extrapolation, and visualization.

2.2 Research Variables

This study involves two types of variables: primary and secondary. The primary variable is the number of malaria cases, which are available for all regencies and municipalities (districts/cities) in Papua Province. However, for spatial analysis, only five regencies/municipalities could be utilized due to the availability of rainfall data as the secondary variable. Subsequently, this study extrapolates the number of malaria cases in regencies/municipalities of Central Papua Province, a newly established region separated from Papua Province, by leveraging spatial information from Papua Province. The definitions of each variable used in the study are shown in Table 1.

Table 1. Definition of Variables

No.	Variable	Definition	Unit
1	Primary Variable	Number Of Malaria Cases Per 1,000 Population	Cases Per 1,000 Population
2	Secondary Variable	Annual Rainfall Amount	Millimeters (mm/Year)
3	Distance Variable	Geographic Coordinates (Longitude and Latitude) Of Each Region	Decimal Degrees (°)

2.3 Auto-Covariance and Cross-Covariance Experimental

The co-kriging method requires the use of a multivariate covariance matrix to delineate the spatial relationship between multiple variables. Reference by Vargas-Guzmán and Yeh [17], a set of historical data is denoted by p and a set of contemporary data is denoted by s, with the former located at the location m. The numerical multivariate covariance matrix for attributes $\{z, w, \dots, q\}$ is given by:

$$\boldsymbol{C}_{pp} = \begin{bmatrix} \boldsymbol{c}_{z_p z_p} & \boldsymbol{c}_{z_p w_p} & \cdots & \boldsymbol{c}_{z_p q_p} \\ \boldsymbol{c}_{w_p z_p} & \boldsymbol{c}_{w_p w_p} & \cdots & \boldsymbol{c}_{w_p q_p} \\ \vdots & \vdots & \ddots & \vdots \\ \boldsymbol{c}_{q_p z_p} & \boldsymbol{c}_{q_p w_p} & \cdots & \boldsymbol{c}_{q_p q_p} \end{bmatrix}, \boldsymbol{C}_{ss} = \begin{bmatrix} \boldsymbol{c}_{z_s z_s} & \boldsymbol{c}_{z_s w_s} & \cdots & \boldsymbol{c}_{z_s q_s} \\ \boldsymbol{c}_{w_s z_s} & \boldsymbol{c}_{w_s w_s} & \cdots & \boldsymbol{c}_{w_s q_s} \\ \vdots & \vdots & \ddots & \vdots \\ \boldsymbol{c}_{q_s z_s} & \boldsymbol{c}_{q_s w_s} & \cdots & \boldsymbol{c}_{q_s q_s} \end{bmatrix},$$

$$\boldsymbol{C}_{ps} = \begin{bmatrix} \boldsymbol{c}_{z_p z_s} & \boldsymbol{c}_{z_p w_s} & \cdots & \boldsymbol{c}_{z_p q_s} \\ \boldsymbol{c}_{w_p z_s} & \boldsymbol{c}_{w_p w_s} & \cdots & \boldsymbol{c}_{w_p q_s} \\ \vdots & \vdots & \ddots & \vdots \\ \boldsymbol{c}_{q_p z_s} & \boldsymbol{c}_{q_p w_s} & \cdots & \boldsymbol{c}_{q_p q_s} \end{bmatrix}.$$

In this context, C (capitalised) denotes a multivariate covariance matrix. Of the three matrices under consideration, it is evident that all diagonal elements correspond to auto-covariance matrices, while elements external to the diagonal correspond to cross-covariance matrices. The formula for the covariance between the data and the location to be estimated is as follows:

$$\boldsymbol{C}_{p0} = \begin{bmatrix} \vec{\boldsymbol{c}}_{z_p z_0} & \vec{\boldsymbol{c}}_{z_p w_0} & \cdots & \vec{\boldsymbol{c}}_{z_p q_0} \\ \vec{\boldsymbol{c}}_{w_p z_0} & \vec{\boldsymbol{c}}_{w_p w_0} & \cdots & \vec{\boldsymbol{c}}_{w_p q_0} \\ \vdots & \vdots & \ddots & \vdots \\ \vec{\boldsymbol{c}}_{q_p z_0} & \vec{\boldsymbol{c}}_{q_p w_0} & \cdots & \vec{\boldsymbol{c}}_{q_p q_0} \end{bmatrix}, \quad \boldsymbol{C}_{s0} = \begin{bmatrix} \vec{\boldsymbol{c}}_{z_s z_0} & \vec{\boldsymbol{c}}_{z_s w_0} & \cdots & \vec{\boldsymbol{c}}_{z_s q_0} \\ \vec{\boldsymbol{c}}_{w_s z_0} & \vec{\boldsymbol{c}}_{w_s w_0} & \cdots & \vec{\boldsymbol{c}}_{w_s q_0} \\ \vdots & \vdots & \ddots & \vdots \\ \vec{\boldsymbol{c}}_{q_s z_0} & \vec{\boldsymbol{c}}_{q_s w_0} & \cdots & \vec{\boldsymbol{c}}_{q_s q_0} \end{bmatrix}.$$

2.4 Theoretical Covariance

Theoretical covariance functions define valid multivariate spatial dependencies by ensuring that both marginal and cross-covariances lead to a nonnegative definite covariance matrix. These functions are essential for modeling multivariate spatial fields, particularly when incorporating cross-dependence between variables in co-kriging and simulation models [18]. In the field of co-kriging analysis, there are three theoretical covariance models that are frequently employed: the spherical model, the exponential model, and the Gaussian model [19]. The forms of these three models can be defined as follows:

1. Spherical

$$C(h) = \begin{cases} P+Q & ;h=0 \\ (P+Q)\left[1 - 1{,}5\left(\frac{h}{r}\right) - 0{,}5\left(\frac{h}{r}\right)^3\right] & ;0 \le h \le r \\ 0 & ;h > r \end{cases}. \quad (1)$$

2. Exponential

$$C(h) = (P+Q)\left[1 - exp\ exp\left(-\frac{h}{r}\right)\right]. \quad (2)$$

3. Gaussian

$$C(h) = (P+Q)\left[1 - exp\ exp\left(-\frac{h}{r}\right)^2\right]. \quad (3)$$

P (nugget effect) refers to the estimated auto-covariance and cross-covariance values at very small distances close to zero. Q (sill) represents the highest value attained by the auto-covariance and cross-covariance. Meanwhile, r (range) indicates the distance at which the covariance reaches this maximum value.

2.5 Co-Kriging Method

Co-kriging is a spatial interpolation method that utilises the spatial dependence between the primary and secondary variables [20]. Primary variables are defined as the principal variables employed for interpolation, while secondary variables are designated as covariates. Co-kriging estimates are defined as linear combinations of primary and secondary variables, as previously defined [21].

$$\hat{u}_0 = \sum_{i=1}^{n} \alpha_i u_i + \sum_{i=1}^{m} \beta_j v_j\,, \quad (4)$$

when $\sum_{i=1}^{n} \alpha_i = 1$ and $\sum_{i=1}^{m} \beta_j = 0$, and where:

$\hat{u}_0$: the estimated value of U at location 0;
$u_1, \ldots, u_n$: secondary variable data at n locations;
$v_1, \ldots, v_m$: secondary variable data at m locations;
α_i and β_j : co-kriging weighting value.

In ordinary co-kriging, as illustrated in Eq. (4), the function $\hat{u}_i$, which is linear at points $\hat{u}_1, \ldots, \hat{u}_n$, is also unbiased and minimizes the mean squared error of the estimate. In accordance with the unbiasedness condition stipulated in Eq. (4), the error estimator is derived in Eq. (5).

$$Q = \hat{U}_0 - U_0 = \sum_{i=1}^{n} \alpha_i U_i + \sum_{i=1}^{m} \beta_j V_j - U_0 \quad (5)$$

The equation given by Eq. (5) can be converted into matrix form by employing the notation provided in Eq. (6).

$$Q = \boldsymbol{\omega}^t \boldsymbol{Z} \quad (6)$$

The equation for the variance of the error estimator in co-kriging weighting and covariance between random variables is given in Eq. (7).

$$Var(Q) = \boldsymbol{\omega}^t \boldsymbol{C}_Z \boldsymbol{\omega} \quad (7)$$

$\boldsymbol{C_Z}$ denotes the covariance matrix of $\boldsymbol{Z}$. Pursuant to the expansion of Eq. (7), the variance of the error estimate of the co-kriging weight and the variance between random variables can be expressed in Eq. (8).

$$Var\,(Q) = Var\left[\sum_{i=1}^{n}\alpha_i U_i + \sum_{i=1}^{m}\beta_j V_j - U_0\right]. \tag{8}$$

In order to produce weights that minimise error variance and satisfy the unbiasedness condition, it is necessary to minimise the two constraint functions using the Lagrange multiplier method. Each unbiased condition is then multiplied by the Lagrange multiplier, and the resultant sum is added to Eq. (8). This process ultimately results in Eq. (9).

$$L = \boldsymbol{\omega^t C_Z \omega} + 2\mu_1\left(\sum_{i=1}^{n}\alpha_i - 1\right) + 2\mu_2\left(\sum_{i=1}^{m}\beta_i\right). \tag{9}$$

Matrix equations can be formed from covariance matrices or from semivariograms $\gamma(h)$, where $\gamma(h)$ denotes the semivariogram function that quantifies spatial dependence at distance h. When semivariogram matrices are used, the parameters $\lambda_1, \ldots, \lambda_n$ representing the Lagrange multipliers that enforce unbiasedness in the Co-Kriging estimator must be optimized according to Eq. (10).

$$LQ = X^{-1}Y, \tag{10}$$

X represents the covariance matrix that captures the relationship between the primary and secondary variables across different observation locations. Therefore, the matrix equation is equivalent to that given in Eq. (11).

$$\begin{bmatrix}\alpha_1\\ \vdots\\ \alpha_n\\ \beta_1\\ \vdots\\ \beta_m\\ \mu_1\\ \mu_2\end{bmatrix} = \begin{bmatrix} Cov(U_1U_1) & \cdots & Cov(U_1U_n) & Cov(U_1V_1) & \vdots & Cov(U_1V_m) & 1 & 0\\ \vdots & \ddots & \vdots & \vdots & \ddots & \vdots & \vdots & \vdots\\ Cov(U_nU_1) & \cdots & Cov(U_nU_n) & Cov(U_nV_1) & \cdots & Cov(U_nV_m) & 1 & 0\\ Cov(V_1U_1) & \cdots & Cov(V_1U_n) & Cov(V_1V_1) & \cdots & Cov(V_1V_m) & 0 & 1\\ \vdots & \ddots & \vdots & \vdots & \ddots & \vdots & \vdots & \vdots\\ Cov(V_mU_1) & \cdots & Cov(V_mU_n) & Cov(V_mV_1) & \cdots & Cov(V_mV_m) & 0 & 1\\ 1 & \cdots & 1 & 0 & \cdots & 0 & 0 & 1\\ 0 & \cdots & 0 & 1 & \cdots & 1 & 0 & 0\end{bmatrix}^{-1}\begin{bmatrix} Cov(U_0U_1)\\ \vdots\\ Cov(U_0U_n)\\ Cov(U_0V_1)\\ \vdots\\ Cov(U_0U_m)\\ 1\\ 0\end{bmatrix}. \tag{11}$$

2.6 Cross-Validation

Cross-validation is a methodological framework for the evaluation of interpolation accuracy, providing a more reliable approach than a mere analysis of error. Cross-validation can be categorised into three distinct types: the Holdout Method, K-Fold Cross-Validation, and Leave-One-Out Cross-Validation (LOOCV). In this study, the difference between the actual data used for modeling and the estimated data will be examined using the following calculation.

1. The mean-squared error (MSE) is a statistical metric that calculates the mean of the squares of the deviations between the observed values and the estimated values. The formula for MSE is as follows.

$$\text{MSE} = \sum_{i=1}^{n}\frac{Z(x_i) - \hat{Z}(x_i))^2}{n}. \tag{12}$$

2. The Mean Absolute Percentage Error (MAPE) is a metric used to evaluate forecasting accuracy by comparing the absolute percentage difference between actual and predicted values. Lower MAPE values indicate better model performance, with standard interpretive ranges used to assess prediction quality [22].

$$\text{MAPE} = \frac{100\%}{n}\sum_{i=1}^{n}\left|\frac{actual - forecast}{actual}\right|. \tag{13}$$

In the context of Co-Kriging, the formula for MAPE is as follows.

$$MAPE = \frac{100\%}{n}\sum_{i=1}^{n}\left|\frac{Z(x_i) - \hat{Z}(x_i)}{Z(x_i)}\right|, \quad (14)$$

where $Z(x_i)$ is the observed value at location (x_i); $\hat{Z}(x_i)$ is the Co-Kriging predicted value at location (x_i); n is the number of observation points.

2.7 Data Analysis Steps

1. Displays data on malaria cases and rainfall in Papua Province.
2. The following study will test the goodness of fit of the Co-Kriging model with spherical semivariogram on data on the number of malaria cases affected by rainfall in Papua Province. The objective of this test is to ascertain the extent to which the spherical semivariogram model successfully represents spatial relationships. The following steps are involved in this process:
   a. The formation of a distance matrix between observation locations can be accomplished through the application of the following equation:

   $$h_{ij} = \sqrt{(x_i - x_j)^2 + (y_i - y_j)^2} \quad (15)$$

   In this study, x and y represent the longitude and latitude coordinates of locations i and j, respectively.
   b. The estimation of the location is to be performed using the following equation:

   $$h_{i0} = \sqrt{(x_i - x_0)^2 + (y_i - y_0)^2} \quad (16)$$

   In order to estimate the value of the location, x_0 and y_0 are required, which are the coordinates of the location in this case. These are the regencies/cities in Central Papua Province.
   c. The experimental auto-covariance and cross-covariance between the primary variable (malaria cases) and secondary variable (rainfall), namely $C(h)$, were calculated.
   d. The distance between locations is to be plotted against the experimental covariance value, and the result is to be adjusted to the spherical semivariogram theoretical model.
3. The following steps are taken in order to estimate the Co-Kriging model on data on the number of malaria cases affected by rainfall in Papua Province:
   a. The formation of a covariance matrix between locations for primary and secondary variables, as well as a covariance matrix between estimated locations and observed locations, is symbolised by C.
   b. The inverse of the covariance matrix of the observation locations must be calculated.
   c. The weight of the Co-Kriging estimation is calculated based on the results of matrix inversion and the covariance between locations.
   d. The estimation of the value of the primary variable (malaria cases) at unobserved locations is achieved through the implementation of Co-Kriging calculation weights.
   e. Model Selection Through Accuracy Evaluation. After estimating the values of the primary variable (malaria cases) at unobserved locations, follow these steps to evaluate and select the best model:
      i. The MAPE is calculated as follows: The MAPE is a metric used to quantify the discrepancy between estimated and actual values, assuming such data is available for validation purposes.
      ii. Calculate MSE: Compute MSE to measure the average squared error between the estimated values and the actual values.
      iii. Compare MAPE and MSE values: Select the model that yields the smallest MAPE and MSE values, indicating higher estimation accuracy.

3. RESULTS AND DISCUSSION

Spatial extrapolation using the Co-Kriging method reveals that regions in Central Papua with higher levels of rainfall tend to exhibit elevated estimates of malaria incidence. This estimation is based on observational malaria data from Papua Province combined with rainfall information, allowing for predictions in data-scarce areas such as Central Papua. The resulting spatial pattern is consistent with previous research conducted in tropical settings, which demonstrates that increased rainfall facilitates the formation of mosquito breeding sites and thereby enhances malaria transmission risk [23]-[27]. The integration of rainfall as a secondary variable in the Co-Kriging framework enhances the accuracy of spatial predictions by capturing key environmental drivers of disease transmission. These findings provide a robust basis for understanding malaria distribution patterns in Central Papua and support the use of geostatistical approaches for informing targeted public health interventions.

3.1 Descriptive Statistics

To provide an overview of the data used in this study, descriptive statistics were applied. These measures offer an understanding of the central values and the dispersion of the observed variables. The summary of these statistics is shown in Table 2.

Table 2. Descriptive Statistics

Variable	N	Min.	Max.	Mean	Standard Deviation
Annual Rainfall (mm/year)	5	1,583.7	2902.6	2,266.76	632.6673
Malaria Cases (per 1000 population)	5	19.45	317.29	204.052	132.4924

Based on the descriptive statistical analysis, it is shown that the average annual rainfall in Papua Province is 2,266.76 mm, with a standard deviation of 632.6673 mm. This indicates that Papua experiences a high level of rainfall, which is consistent with its tropical climate [28], [29]. High rainfall can create more stagnant water, which serves as breeding grounds for mosquitoes, potentially increasing the risk of malaria transmission. Furthermore, the average number of malaria cases per 1,000 population is 204.052, with a standard deviation of 132.4924. This relatively high number suggests that malaria remains a significant public health concern in the region.

According to Fig. 1, the spatial distribution of malaria cases in Papua Province exhibits considerable regional variation. The regencies of Mamberamo Raya and Keerom, located in the central-northern and northeastern areas, record the highest incidence rates exceeding 500 cases per 1,000 population—represented by the darkest shades on the map. Sarmi, Jayapura, and Kota Jayapura in the central-eastern region show slightly lower yet still elevated rates of approximately 300 to 400 per 1,000. In contrast, Waropen in the southwest displays moderate incidence levels (150–250 per 1,000), while the northern islands, such as Kepulauan Yapen, Biak Numfor, and Supiori, demonstrate the lowest burden, with fewer than 100 cases per 1,000 population, as indicated by the lightest color. This spatial variability suggests that environmental factors, such as rainfall patterns and the presence of stagnant water, along with the accessibility and effectiveness of vector control programs, play a significant role in influencing malaria transmission.

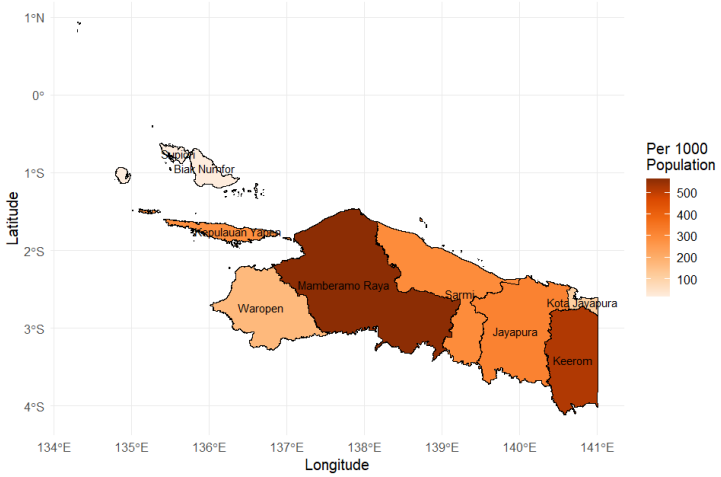

Figure 1. Spatial Distribution of Malaria Incidence in Papua Province (per 1,000 Population)

3.2 Experimental Semivariogram

The estimation process for malaria cases begins with utilizing spatial data from various districts across Papua Province. The first step involves calculating the distance (h) between district centroids within Papua, as well as the distance between those districts and a target location in Central Papua for which estimates are to be made. This computation was performed using Python-based geospatial analysis tools. Once the pairwise distances were obtained, they were grouped into discrete distance classes for semivariogram modeling. In this study, the distances were divided into four classes. Unlike traditional methods such as Sturges' rule, commonly applied to large spatial datasets, this study opted not to use such classical binning techniques. As argued by Shimazaki and Shinomoto [30], traditional approaches often fall short when dealing with sparse or spatially irregular data, as they fail to account for fluctuations and local heterogeneity. The resulting classification produced 25 distance pairs within each class, which served as the basis for constructing the empirical semivariogram.

Table 3. Distance Class Grouping and Experimental Covariance

Class Interval	Distance (h)	N	Auto-Covariance U	Auto-Covariance V	Cross-Covariance U-V
0.00000-1.240940	0.62047	11	0.485009	0.292763	0.102132
1.24104-2.482080	1.86156	2	-0.600020	0.194874	-0.391883
2.48208-3.723120	3.10260	4	-326467	-0.108040	-0.283643
3.72312-4.964159	4.34364	8	-0.031779	0.044775	0.099360

Following the acquisition of the experimental auto-covariance and cross-covariance values. The subsequent step is to identify the most appropriate models by fitting several theoretical covariance structures. such as the spherical. exponential. and Gaussian functions. As outlined in Eqs. (1), (2), and (3), this modeling procedure necessitates the estimation of three key parameters: P (nugget effect), Q (sill), and r (range). The parameter values for the auto-covariance function are inferred from the distance versus experimental auto-covariance plot. while those for the cross-covariance function are derived from the corresponding cross-covariance plot. Fig. 2 displays the distance-based experimental auto-covariance plot for the first variable, representing districts or cities within Papua Province.

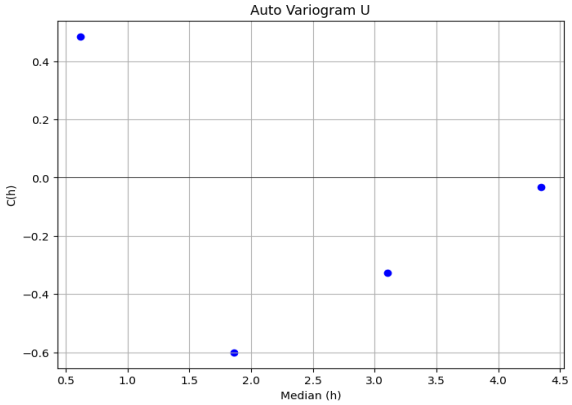

Figure 2. Plot of Distance Versus Experimental Auto Covariance for the Malaria Variable

As illustrated in Fig. 2, the estimated parameter values for modeling the auto-covariance of the district/city-level malaria variable are $P = 0.485008$, $Q = 0.48500$, and $r = 0.620469$. Meanwhile, the plot depicting the relationship between distance and experimental auto-covariance for the second variable (Station) is provided in Fig. 3 below.

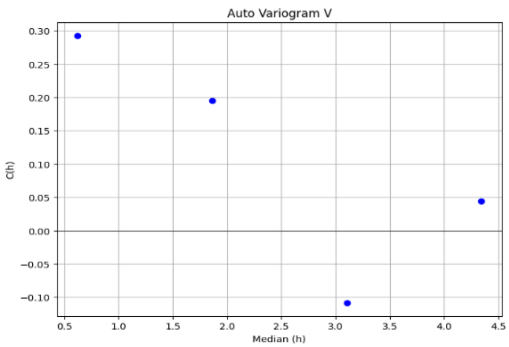

Figure 3. Plot of Distance Versus Experimental Auto-Covariance for the Rainfall Variable

As shown in Fig. 3, the estimated values for the auto-covariance model of the Station variable are $P = 0.044774$, $Q = 0.292763$, and $r = 0.620469$. The following plot in Fig. 4 depicts how the experimental cross-covariance between the first and second variables changes with distance.

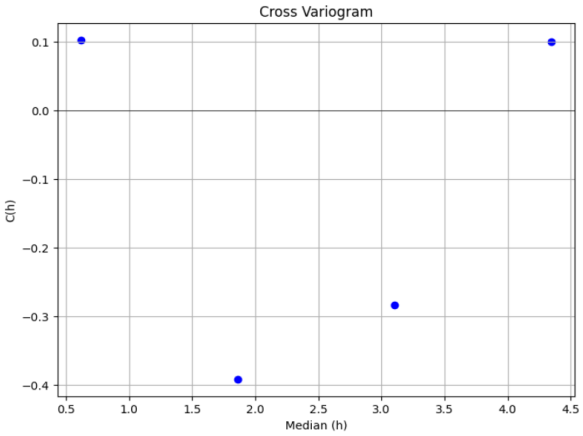

Figure 4. Plot of Distance Versus Experimental Cross-Covariance

Referring to Fig. 4, the estimated values of the parameters used to represent the cross-covariance between the first and second variables are $P = 0.09936$, $Q = 0.10213$, and $r = 0.620469$.

3.3 Theoretical Semivariogram

Following the estimation of the parameters P, Q, and r from each covariance structure, the spherical model can be expressed using Eq. (1), as detailed below.

Spherical auto-covariance function for the primary variable (malaria cases):

$$C_U(h) = \begin{cases} (0.48501 + 0.48501), & 0 = h; \\ (0.48501 + 0.48501)\left(1 - \dfrac{3h}{2(0.62047)} + \dfrac{h^3}{2(0.62047)^2}\right), & 0 < h \leq 0.62047; \\ 0, & h > 0.62047. \end{cases} \quad (17)$$

Spherical auto-covariance function for the secondary variable (rainfall):

$$C_V(h) = \begin{cases} (0.044775 + 0.2927634), & 0 = h; \\ (0.044775 + 0.2927634)\left(1 - \dfrac{3h}{2(0.62047)} + \dfrac{h^3}{2(0.62047)^2}\right), & 0 < h \leq 0.62047; \\ 0, & h > 0.62047. \end{cases} \quad (18)$$

Spherical cross-covariance function:

$$C_V(h) = \begin{cases} (0.09936 + 0.10213), & 0 = h; \\ (0.09936 + 0.10213)\left(1 - \dfrac{3h}{2(0.62047)} + \dfrac{h^3}{2(0.62047)^2}\right), & 0 < h \leq 0.62047; \\ 0, & h > 0.62047. \end{cases} \quad (19)$$

After determining the values of P, Q, and r, The corresponding exponential model is formulated using Eq. (2) as follows:

Exponential auto-covariance function for the primary variable (malaria cases):

$$C(h) = (0.48501 + 0.48501)\left(1 - exp\ exp\ \left(-\frac{h}{0.62047}\right)\right). \quad (20)$$

Exponential auto-covariance function for the secondary variable (rainfall):

$$C(h) = (0.044775 + 0.2927634)\left(1 - exp\ exp\ \left(-\frac{h}{0.62047}\right)\right). \quad (21)$$

Exponential cross-covariance function:

$$C(h) = (0.09936 + 0.10213)\left(1 - exp\ exp\ \left(-\frac{h}{0.62047}\right)\right). \quad (22)$$

Once the values of P, Q, and r have been obtained, the Gaussian model is applied according to Eq. (3), as outlined below:

Gaussian auto-covariance function for the primary variable (malaria cases):

$$C(h) = (0.48501 + 0.48501)\left(1 - exp\ exp\ \left(-\frac{h}{0.62047}\right)^2\right) \quad (23)$$

Gaussian auto-covariance function for the secondary variable (rainfall):

$$C(h) = (0.044775 + 0.2927634)\left(1 - exp\ exp\ \left(-\frac{h}{0.62047}\right)^2\right) \quad (24)$$

Gaussian cross-covariance function:

$$C(h) = (0.09936 + 0.10213)\left(1 - exp\ exp\ \left(-\frac{h}{0.62047}\right)^2\right) \quad (25)$$

3.4 Comparison of Semivariogram Model

1. Spherical Semivariogram Model

   In the semivariogram analysis, the spherical semivariogram model was employed to generate predicted values, which are presented in Table 4 below.

Table 4. Prediction Results of the Spherical Semivariogram Model

No.	Location	Predicted Data (Z_0)	Actual Data
1.	Jayapura	317.29	317.29
2.	Kepulauan Yapen	283.99	283.99
3.	Biak Numfor	19.45	19.45
4.	Sarmi	291.66	291.66
5.	Kota Jayapura	108.87	107.87

Using the spherical semivariogram model, the MSE was found to be 8.985974×10^{-18} and the MAPE was 3.666353×10^{-9}. Predictions generated by this model are considered highly accurate, as indicated by the extremely low MSE and MAPE values, which approach zero. This suggests that the difference between predicted and actual values is nearly negligible.

However, such exceptionally high accuracy may indicate the presence of overfitting. a condition in which the model is excessively adapted to the training dataset, which hampers its ability to generalize to new inputs. This issue has been identified that semivariogram models with default parameters in kriging interpolation can produce unrealistic spatial patterns, such as extreme rainfall gradients within a narrow radius, which are characteristic of overfitting [31].

Similarly, research by Arétouyap *et al.* [32] demonstrated that inappropriate selection of a semivariogram model can significantly affect prediction outcomes. Therefore, in semivariogram modeling for co-kriging, it is crucial not only to consider low statistical error values but also to evaluate the spatial plausibility and model stability to avoid overfitting and ensure good generalizability.

2. Exponential Semivariogram Model

   In the semivariogram analysis, the exponential semivariogram model was used to generate predicted values, which are presented in Table 5.

Table 5. Prediction Results of the Exponential Semivariogram Model

No.	Location	Predicted Data (Z_0)	Actual Data
1.	Jayapura	325.554728	317.29
2.	Kepulauan Yapen	292.254728	283.99
3.	Biak Numfor	27.714728	19.45
4.	Sarmi	299.924728	291.66
5.	Kota Jayapura	116.134728	107.87

Using the exponential semivariogram model, the MSE was found to be 68.305723, and the MAPE was 11.700522%. The predictions generated by this model are considered reliable, as the MAPE value falls within the acceptable range of 10% to 20%, which indicates good forecasting accuracy [33]. This indicates that the level of prediction error is still within a tolerable threshold.

3. Gaussian Semivariogram Model

In the semivariogram analysis, the Gaussian semivariogram model was used to obtain prediction values, as presented in Table 6.

Table 6. Prediction Results of the Gaussian Semivariogram Model

No.	Location	Predicted Data (Z_0)	Actual Data
1.	Jayapura	320.590758	317.29
2.	Kepulauan Yapen	287.290758	283.99
3.	Biak Numfor	22.750758	19.45
4.	Sarmi	294.960758	291.66
5.	Kota Jayapura	111.170758	107.87

Using the Gaussian semivariogram model, the MSE was found to be 10.895003, and the MAPE was 4.672942%. The predictions produced by this model are considered highly accurate, as the MAPE value is below 10%. This indicates that the Gaussian semivariogram model has excellent predictive capability with a low error rate, making it a highly suitable choice for use.

3.5 Selection of the Best Semivariogram Model

The best semivariogram model for co-kriging interpolation is selected based on a comparison of the MSE and MAPE values derived from the predicted number of malaria cases. The comparison results of the MSE and MAPE values are presented in Table 7.

Table 7. Comparison of MSE and MAPE Values for Semivariogram Models

Semivariogram Model	MSE	MAPE
Spherical	8.985974×10^{-18}	3.666353×10^{-9}%
Exponential	68.30572	11.70052%
Gaussian	10.89500	4.672942%

Based on Table 7, the spherical semivariogram model indeed shows the lowest MSE and MAPE values. However, these values are extremely close to zero, indicating a potential overfitting issue, where the model fits the training data almost perfectly but may generalize poorly to new or unseen data, similar to the overfitting and overestimation challenges highlighted in landslide susceptibility modeling studies [34]. Such overfitting can compromise the model's ability to generalize to unobserved locations, leading to inaccurate predictions at new points.

On the other hand, the Gaussian model produces relatively low MSE and MAPE values that are more spatially reasonable. Therefore, the Gaussian semivariogram model is selected as the best model for co-kriging interpolation in predicting malaria case counts. This is because it yields low error values while remaining within acceptable limits, and it demonstrates better generalization performance compared to the other models.

3.6 Extrapolation Using Co-Kriging

Utilizing the best-performing model, specifically the Gaussian semivariogram, a predictive map illustrating malaria case counts in Central Papua was generated, as depicted in Fig. 5.

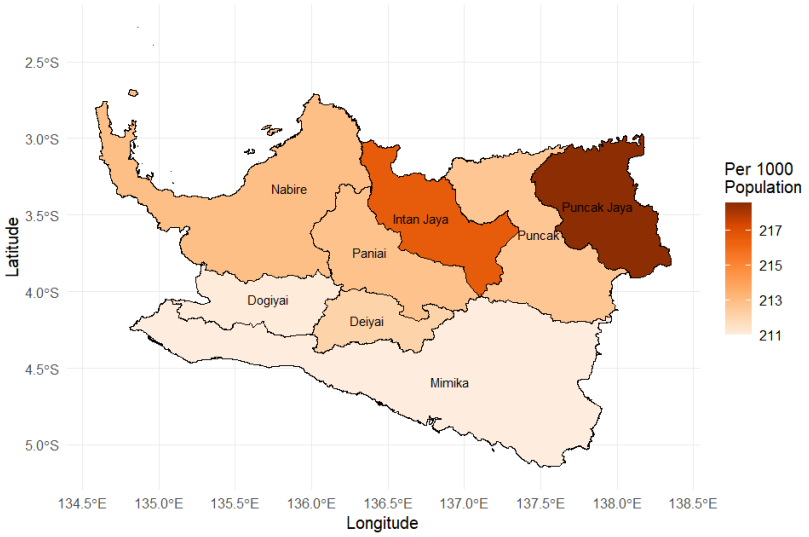

Figure 5. Prediction Map of Malaria Cases in Central Papua

Based on the estimated number of malaria cases in the eight regencies/cities within Central Papua, using observational data from Papua Province, it is shown that the case numbers do not differ significantly. The highest number of cases is found in Puncak Jaya Regency, with 219 cases per 1,000 inhabitants, while the lowest number of cases is in Mimika Regency, with 211 cases per 1,000 inhabitants. The following map presents the combined malaria case distribution for Papua Province and Central Papua by regency/city.

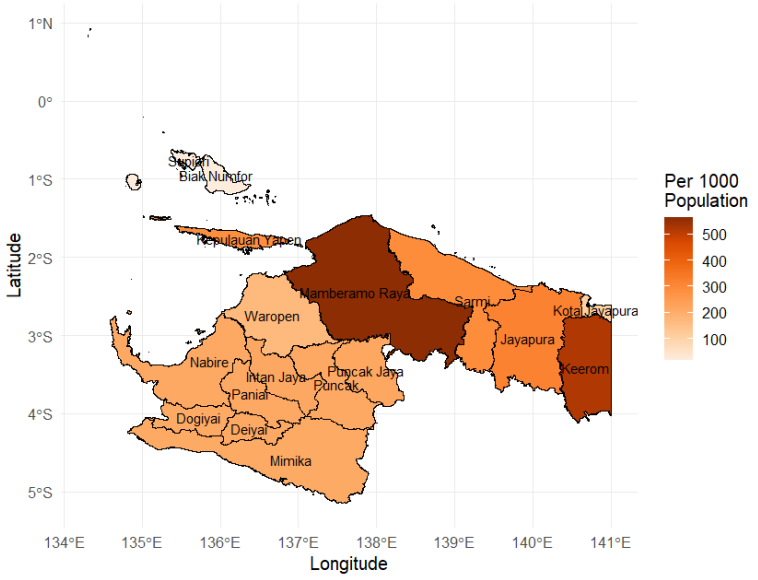

Figure 6. Combined Map of Papua Province and Central Papua

The figure shows the spatial distribution of malaria cases in Papua Province per 1,000 population, with the highest incidence in Mamberamo Raya and Keerom districts (>500 cases) and the lowest in Biak Numfor and Yapen Islands (<100 cases). These results are consistent with estimation using the rainfall-based Co-Kriging method, where the Gaussian model was selected as the best model with MSE 10.895 and MAPE 4.67%. This finding is in line with previous studies showing that Co-Kriging is effective in mapping the distribution of vector-based diseases, as it is able to incorporate environmental variables such as rainfall to improve the accuracy of spatial predictions [11], [12].

4. CONCLUSION

This study successfully implemented the Co-Kriging method by utilizing malaria case data as the main variable and rainfall data as a supporting variable to estimate the number of malaria cases in areas that do not

have data, especially in Central Papua Province. From the evaluation results of three types of semivariogram models, namely, spherical, exponential, and Gaussian. The Gaussian model was identified as the most optimal, indicated by a Mean Squared Error (MSE) value of 10.895 and a Mean Absolute Percentage Error (MAPE) of 4.67%. which reflects excellent predictive performance while remaining realistic. The estimates indicate that the distribution of malaria cases across districts/municipalities in Central Papua is fairly even, with the highest rates found in Puncak Jaya district and the lowest in Mimika district. These findings provide an important initial basis for planning more targeted and spatially-based health interventions.

Author Contributions

Toha Saifudin: Conceptualization, Methodology, and Formal Analysis. Nur Chamidah: Data Curation, Investigation, and Supervision. Azizah Atsariyyah Zhafira: Formal Analysis, Validation, and Writing—Review and Editing. Gabriella Agnes Budijono: Data Curation, Software Development, and Visualization. Rivaldi Sihite: Investigation, Methodology, Project Administration, and Writing—Review and Editing. Mochammad Baihaqi: Software Development and Validation. R. Arya Januarta: Writing—Review and Editing. All authors discussed the results and approved the final version of the manuscript.

Funding Statement

This research received no specific grant from any funding agency in the public, commercial, or not-for-profit sectors.

Acknowledgment

The authors would like to express their sincere gratitude to God Almighty for granting us the strength, inspiration, and perseverance throughout the completion of this research. The authors also extend their deepest appreciation to Universitas Airlangga, especially the Statistics Study Program, Faculty of Science and Technology, for providing academic support and facilities essential to this study. Special thanks are conveyed to our supervising lecturers for their continuous guidance, insightful feedback, and valuable encouragement during the research process. We are also grateful to Badan Pusat Statistik (BPS) Provinsi Papua for providing access to the data used in this study. Finally, the authors would like to acknowledge their families and peers for their understanding and moral support. Any constructive criticism and suggestions for the improvement of this research are highly welcomed and appreciated.

Declarations

This research is carried out jointly according to the division of tasks of each one, without any conflict between authors.

Declaration of Generative AI and AI-assisted Technologies

Generative AI tools (e.g., ChatGPT) were used solely for language refinement, including grammar, spelling, and clarity. The scientific content, analysis, interpretation, and conclusions were developed entirely by the authors. All final text was reviewed and approved by the authors.

REFERENCES

[1] F. Adugna, M. Wale, E. Nibret, and Z. Ameha, "DENSITY AND SPECIES COMPOSITION OF ANOPHELES MOSQUITO LARVAE ALONG LAKE TANA, NORTHWEST ETHIOPIA," *Sci. African*, vol. 27, no. June 2024, p. e02605, 2025. doi: https://doi.org/10.1016/j.sciaf.2025.e02605.

[2] World Health Organization, "WORLD MALARIA REPORT 2023," 2023. [Online]. Available: https://www.who.int/teams/global-malaria-programme/reports/world-malaria-report-2023

[3] Kementerian Kesehatan Republik Indonesia, "PROFIL KESEHATAN," 2023.

[4] E. E. Nurmala, "DINAMIKA PERUBAHAN UNSUR IKLIM (SUHU, KELEMBABAN DAN CURAH HUJAN) DAN KEJADIAN MALARIA PADA PENDUDUK PANDEGLANG," *J. Dunia Kesmas*, vol. 6, no. 2, pp. 63–69, 2017.

[5] S. Sulasmi, D. E. Setyaningtyas, A. Rosanji, and N. Rahayu, "PENGARUH CURAH HUJAN, KELEMBABAN, DAN TEMPERATUR TERHADAP PREVALENSI MALARIA DI KABUPATEN TANAH BUMBU KALIMANTAN SELATAN," *J. Heal. Epidemiol. Commun. Dis.*, vol. 3, no. 1, pp. 22–27, 2017. doi: https://doi.org/10.22435/jhecds.v3i1.1794.

[6] A. Y. Baidjoe *et al.*, "FACTORS ASSOCIATED WITH HIGH HETEROGENEITY OF MALARIA AT FINE SPATIAL SCALE IN THE WESTERN KENYAN HIGHLANDS," *Malar. J.*, vol. 15, no. 1, pp. 1–9, 2016. doi: https://doi.org/10.1186/s12936-016-1362-y.

[7] T. Mukhopadhyay, S. Chakraborty, S. Dey, S. Adhikari, and R. Chowdhury, "A CRITICAL ASSESSMENT OF KRIGING MODEL VARIANTS FOR HIGH-FIDELITY UNCERTAINTY QUANTIFICATION IN DYNAMICS OF COMPOSITE SHELLS," *Arch Comput. Methods Eng*, vol. 24, no. 3, pp. 495–518, 2017. doi: https://doi.org/10.1007/s11831-016-9178-z.

[8] T. Saifudin, A. Faiza, L. Puspasari, and Z. 'Ilmatun Nurrohmah, "ESTIMATING THE CONCENTRATION OF NO2 WITH THE COKRIGING METHOD IN THE CAPITAL CITY OF JAKARTA," *BAREKENG J. Ilmu Mat. dan Terap.*, vol. 17, no. 4, pp. 1985–1996, 2023. doi: https://doi.org/10.30598/barekengvol17iss4pp1985-1996.

[9] Ishaq, "EFEKTIVITAS ORDINARY COKRIGING DAN KRIGING UNTUK KARAKTERISASI POTENSI MANIFESTASI PANAS BUMI," *J. INTEKNA*, vol. 18, no. 2, pp. 67–131, 2018, [Online]. Available: http://ejurnal.poliban.ac.id/index.php/intekna/issue/archive

[10] A. P. Nugraha, A. Granitio Irwan, and L. Nugraha, "PERBANDINGAN GEOSTATISTIK METODE KRIGING DAN CO-KRIGING MENGGUNAKAN ESTIMASI POINT KRIGING," vol. 2020, pp. 177–181, 2020.

[11] D. Payares-Garcia, F. Osei, J. Mateu, and A. Stein, "A POISSON COKRIGING MODELING OF CO-CIRCULATION OF MOSQUITO-BORNE DISEASES IN COLOMBIA," *Environ. Ecol. Stat.*, vol. 32, no. 1, pp. 149–173, 2025. doi: https://doi.org/10.1007/s10651-025-00646-w.

[12] K. Sheikhzadeh *et al.*, "PREDICTING MALARIA TRANSMISSION RISK IN ENDEMIC AREAS OF IRAN: A MULTILEVEL MODELING USING CLIMATE AND SOCIOECONOMIC INDICATORS," *Iran. Red Crescent Med. J.*, vol. 19, no. 4, 2017. doi: https://doi.org/10.5812/ircmj.45132.

[13] Republik Indonesia, "UNDANG-UNDANG NOMOR 15 TAHUN 2022 TENTANG PEMBENTUKAN PROVINSI PAPUA TENGAH," Jakarta, 2022. [Online]. Available: https://peraturan.bpk.go.id/Details/217798/uu-no-15-tahun-2022

[14] BPS Provinsi Papua, *PROVINSI PAPUA DALAM ANGKA 2025*. 2025.

[15] R Core Team, "R: A LANGUAGE AND ENVIRONMENT FOR STATISTICAL COMPUTING," Vienna, Austria, 2023. [Online]. Available: https://www.r-project.org/

[16] Python Software Foundation, "THE PYTHON LANGUAGE REFERENCE." [Online]. Available: https://docs.python.org/3/reference/

[17] J. A. Vargas-Guzmán and T. C. J. Yeh, "SEQUENTIAL KRIGING AND COKRIGING: TWO POWERFUL GEOSTATISTICAL APPROACHES," *Stoch. Environ. Res. Risk Assess.*, vol. 13, no. 6, pp. 416–435, 1999. doi: https://doi.org/10.1007/s004770050047.

[18] M. G. Genton and W. Kleiber, "CROSS-COVARIANCE FUNCTIONS FOR MULTIVARIATE GEOSTATISTICS," *Stat. Sci.*, vol. 30, no. 2, pp. 147–163, 2015. doi: https://doi.org/10.1214/14-STS487.

[19] E. P. Putra, R. Goejantoro, and S. Suyitno, "PENAKSIRAN KANDUNGAN KLORIDA DI SUNGAI MAHAKAM WILAYAH SAMARINDA TAHUN 2017 DENGAN METODE COKRIGING," *Eksponensial*, vol. 11, no. 2, pp. 175–180, 2020. doi: https://doi.org/10.30872/eksponensial.v11i2.661.

[20] N. Chamidah *et al.*, "PREDICTION AND ANALYSIS OF THE NUMBER OF ARI CASES BASED ON PM 2 . 5 CONCENTRATION WITH CO-KRIGING APPROACH," vol. 8, no. 1, pp. 1–11, 2025. doi: https://doi.org/10.12962/j27213862.v8i1.20512.

[21] T. C. Bailey and A. Gatrell, *INTERACTIVE SPATIAL DATA ANALYSIS*. Pearson Education Limited, 1995.

[22] M. A. Maricar, "ANALISA PERBANDINGAN NILAI AKURASI MOVING AVERAGE DAN EXPONENTIAL SMOOTHING UNTUK SISTEM PERAMALAN PENDAPATAN PADA PERUSAHAAN XYZ," *J. Sist. dan Inform.*, vol. 13, pp. 37–46, 2019.

[23] M. M. Kifle, T. T. Teklemariam, A. M. Teweldeberhan, E. H. Tesfamariam, A. K. Andegiorgish, and E. Azaria Kidane, "MALARIA RISK STRATIFICATION AND MODELING THE EFFECT OF RAINFALL ON MALARIA INCIDENCE IN ERITREA," *J. Environ. Public Health*, vol. 2019, 2019. doi: https://doi.org/10.1155/2019/7314129.

[24] N. Matsushita *et al.*, "DIFFERENCES OF RAINFALL–MALARIA ASSOCIATIONS IN LOWLAND AND HIGHLAND IN WESTERN KENYA," *Int. J. Environ. Res. Public Health*, vol. 16, no. 19, pp. 1–13, 2019. doi: https://doi.org/10.3390/ijerph16193693.

[25] A. Noé, S. I. Zaman, M. Rahman, A. K. Saha, M. M. Aktaruzzaman, and R. J. Maude, "MAPPING THE STABILITY OF MALARIA HOTSPOTS IN BANGLADESH FROM 2013 TO 2016," *Malar. J.*, vol. 17, no. 1, pp. 1–21, 2018. doi: https://doi.org/10.1186/s12936-018-2405-3.

[26] D. Dabaro, Z. Birhanu, A. Negash, D. Hawaria, and D. Yewhalaw, "EFFECTS OF RAINFALL, TEMPERATURE AND TOPOGRAPHY ON MALARIA INCIDENCE IN ELIMINATION TARGETED DISTRICT OF ETHIOPIA," *Malar. J.*, vol. 20, no. 1, pp. 1–10, 2021. doi: https://doi.org/10.1186/s12936-021-03641-1.

[27] H. Hasyim *et al.*, "SPATIAL MODELLING OF MALARIA CASES ASSOCIATED WITH ENVIRONMENTAL FACTORS IN SOUTH SUMATRA, INDONESIA," *Malar. J.*, vol. 17, no. 1, pp. 1–15, 2018. doi: https://doi.org/10.1186/s12936-018-2230-8.

[28] W. Hanandita and G. Tampubolon, "GEOGRAPHY AND SOCIAL DISTRIBUTION OF MALARIA IN INDONESIAN PAPUA: A CROSS-SECTIONAL STUDY," *Int. J. Health Geogr.*, vol. 15, no. 1, pp. 1–15, 2016. doi: https://doi.org/10.1186/s12942-016-0043-y.

[29] O. I. Hutasoit, "ECOLOGICAL STUDY OF CLIMATE EFFECTS ON MALARIA INCIDENCE IN JAYAPURA INDONESIA 2010-2022," *Biosci. Med. J. Biomed. Transl. Res.*, vol. 7, no. 5, pp. 3332–3340, 2023. doi: https://doi.org/10.37275/bsm.v7i5.826.

[30] H. Shimazaki and S. Shinomoto, "A METHOD FOR SELECTING THE BIN SIZE OF A TIME HISTOGRAM," *Neural Comput.*, vol. 19, no. 6, pp. 1503–1527, 2007. doi: https://doi.org/10.1162/neco.2007.19.6.1503.

[31] M. P. Lucas *et al.*, "OPTIMIZING AUTOMATED KRIGING TO IMPROVE SPATIAL INTERPOLATION OF MONTHLY RAINFALL OVER COMPLEX TERRAIN," *J. Hydrometeorol.*, vol. 23, no. 4, pp. 561–572, 2022. doi:

https://doi.org/10.1175/JHM-D-21-0171.1.

[32] Z. Arétouyap, P. Njandjock Nouck, R. Nouayou, F. E. Ghomsi Kemgang, A. D. Piépi Toko, and J. Asfahani, "LESSENING THE ADVERSE EFFECT OF THE SEMIVARIOGRAM MODEL SELECTION ON AN INTERPOLATIVE SURVEY USING KRIGING TECHNIQUE," *Springerplus*, vol. 5, no. 1, 2016. doi: https://doi.org/10.1186/s40064-016-2142-4.

[33] A. Hajjah and Y. N. Marlim, "ANALISIS ERROR TERHADAP PERAMALAN DATA PENJUALAN," *Techno.Com*, vol. 20, no. 1, pp. 1–9, 2021. doi: https://doi.org/10.33633/tc.v20i1.4054.

[34] D. A. M. Atok and S. S. Chai, "ADDRESSING OVERFITTING AND OVERESTIMATION CHALLENGES IN LANDSLIDE SUSCEPTIBILITY MODELING: A CASE STUDY OF PENANG ISLAND, MALAYSIA," *Nat. Hazards*, vol. 121, no. 11, pp. 13577–13604, 2025. doi: https://doi.org/10.1007/s11069-025-07329-6.